

# Supporting Information: Molecular orientation of small carboxylates at the water-air interface

Carolyn J. Moll,<sup>†,‡</sup> Alexander A. Korotkevich,<sup>†,‡</sup> Jan Versluis,<sup>†</sup> and Huib J.  
Bakker<sup>\*,†</sup>

<sup>†</sup>*Amolf, Ultrafast Spectroscopy, Science Park 104 Amsterdam, Netherlands*

<sup>‡</sup>*The authors contribute equally to this paper.*

E-mail: A.Korotkevich@amolf.nl, H.Bakker@amolf.nl

Phone: +31 (0)20 754 7100. Fax: +31 (0)20 754 7290

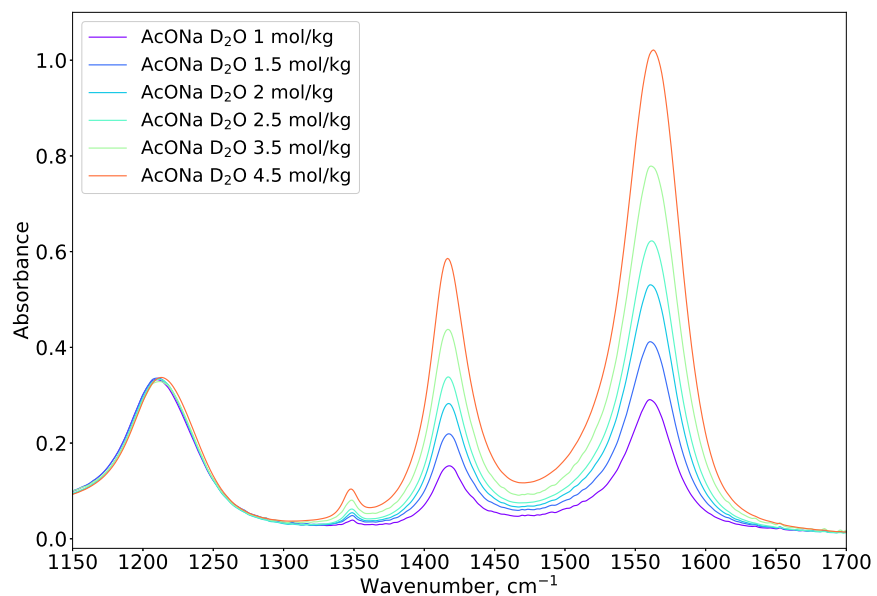


Figure 1: IR absorption spectra in the frequency region within 1150 - 1650  $\text{cm}^{-1}$  of sodium acetate solutions in  $\text{D}_2\text{O}$  in the concentration range of 1.0 - 4.5 m. The spectra are scaled with respect to the bending mode of  $\text{D}_2\text{O}$  appearing at 1210  $\text{cm}^{-1}$

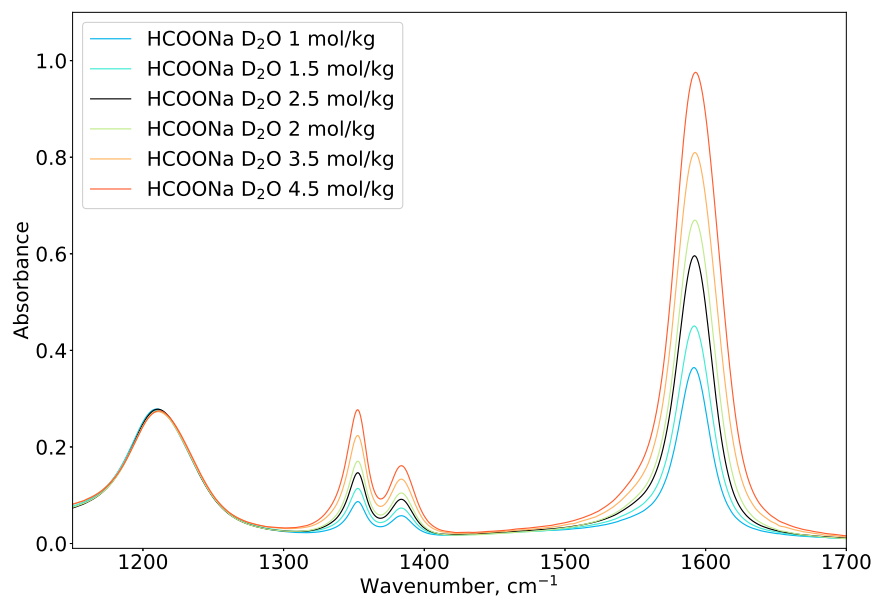


Figure 2: IR absorption spectra in the frequency region within 1150 - 1650  $\text{cm}^{-1}$  of sodium formate solutions in  $\text{D}_2\text{O}$  in the concentration range of 1.0 - 4.5 m. The spectra are scaled with respect to the bending mode of  $\text{D}_2\text{O}$  appearing at 1210  $\text{cm}^{-1}$

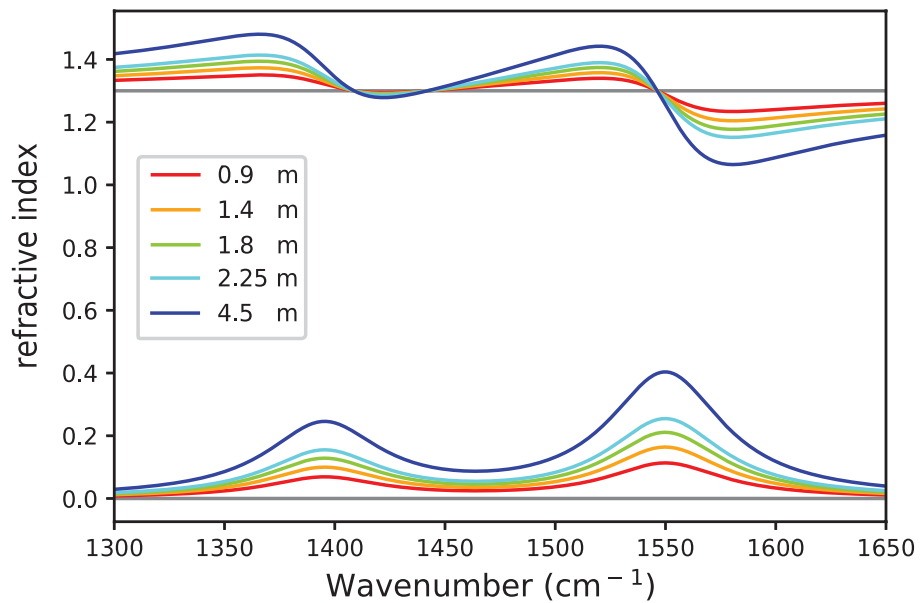


Figure 3: Calculated imaginary (bottom) and real (top) parts of the refractive index in the frequency region  $1300 - 1650 \text{ cm}^{-1}$  of aqueous solution of acetate at different concentrations. The cross-sections of the  $\nu_s$  and  $\nu_{as}$  vibrations of acetate were determined using the known cross-section of the  $\text{D}_2\text{O}$  bending mode centered at  $1210 \text{ cm}^{-1}$ . The real part is calculated using Kramers-Kronig relation.

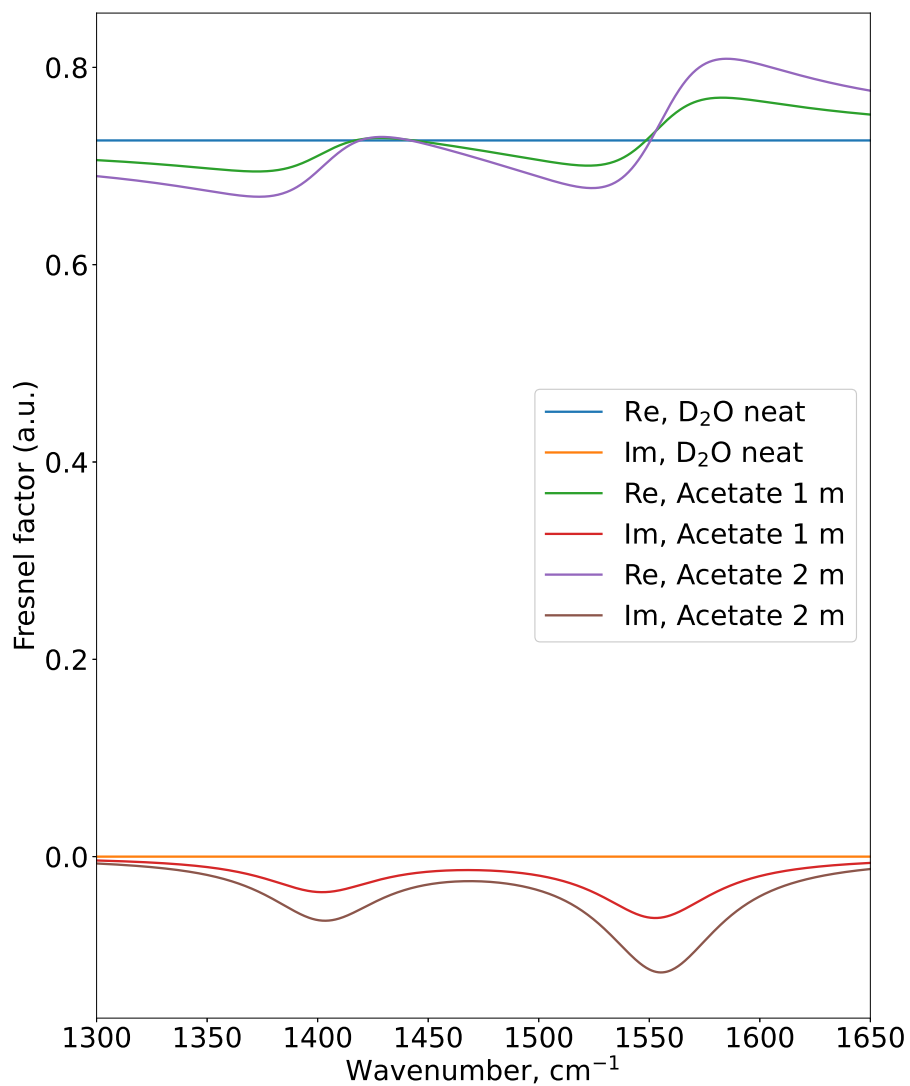


Figure 4: Calculated imaginary (bottom) and real (top) parts of the Fresnel factor in the frequency region 1300 -1650  $\text{cm}^{-1}$  of aqueous solutions of acetate at different concentrations.

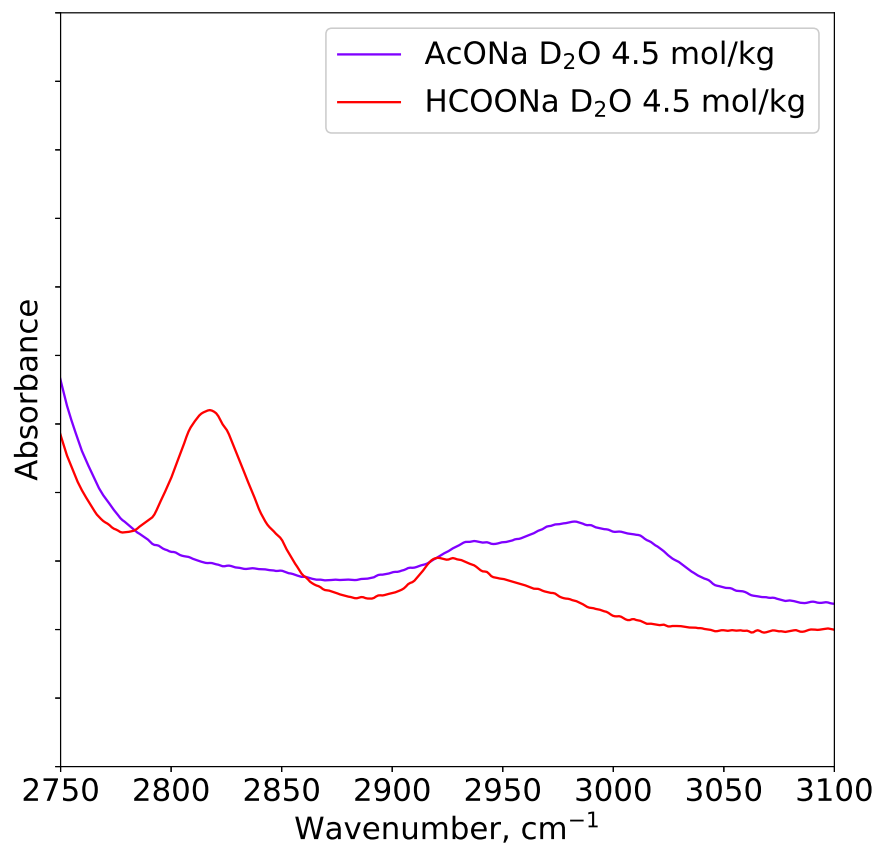


Figure 5: IR absorption spectra in the frequency region 2750 - 3100 cm<sup>-1</sup> of 4.5 m sodium formate and sodium acetate solutions in D<sub>2</sub>O.

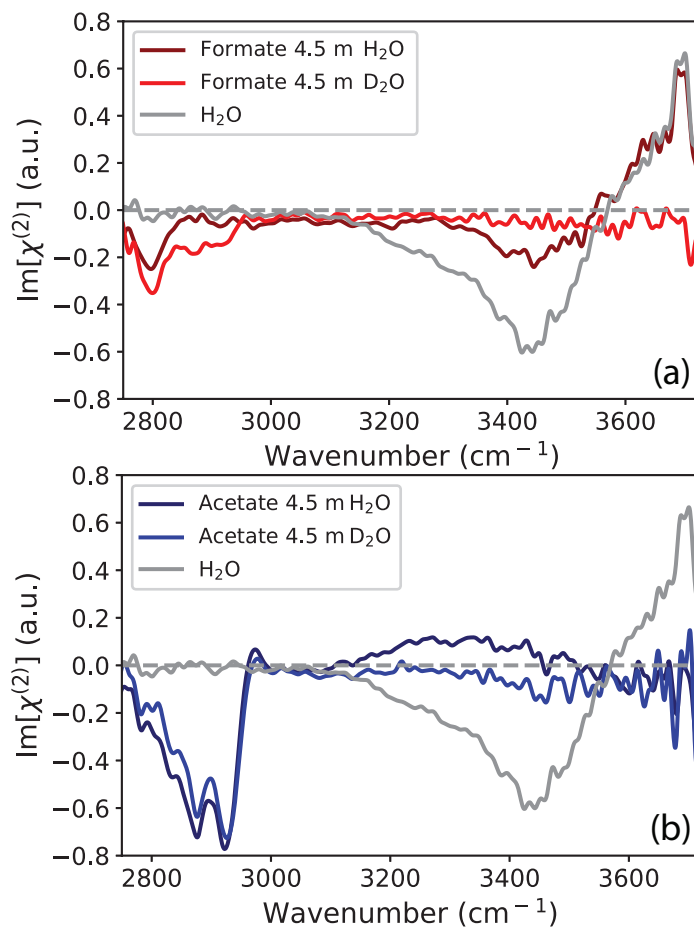


Figure 6: (a)  $\text{Im}[\chi^{(2)}]$  spectra in the frequency region  $2800 - 3720 \text{ cm}^{-1}$  of neat water (gray) and an aqueous formate solution with a concentration of 4.5 m in  $\text{H}_2\text{O}$  (dark red) and  $\text{D}_2\text{O}$  (red). (b)  $\text{Im}[\chi^{(2)}]$  spectra in the frequency region within  $2800 - 3720 \text{ cm}^{-1}$  of neat water (gray) and an aqueous acetate solution with a concentration of 4.5 m in  $\text{H}_2\text{O}$  (dark blue) and  $\text{D}_2\text{O}$  (blue). All measurements are taken in SSP polarization configuration.

The  $\text{Im}[\chi^{(2)}]$  spectrum of the acetate solutions in  $\text{H}_2\text{O}$  and  $\text{D}_2\text{O}$  shows two narrow negative features at  $2880\text{ cm}^{-1}$  and  $2940\text{ cm}^{-1}$  that we assign to the symmetric stretching vibration of the methyl group, ( $\nu_{\text{CH}_3,ss}$ ) and Fermi resonance of the  $\nu_{\text{CH}_3,ss}$  and the overtone of the antisymmetric bending mode of the methyl group, respectively. In addition, the spectra show a narrow positive band at  $3000\text{ cm}^{-1}$  that we assign to the antisymmetric stretching vibration of the methyl group ( $\nu_{\text{CH}_3,as}$ ).<sup>1,2</sup> For formate the  $\text{Im}[\chi^{(2)}]$  spectra show a single negative band in the CH region centered at  $2800\text{ cm}^{-1}$ , which we assign to the stretch vibration of the methine group of the formate ion ( $\nu_{\text{CH}}$ ). The signs of the  $\text{Im}[\chi^{(2)}]$  responses of the  $\nu_{\text{CH}_3,ss}$  and  $\nu_{\text{CH}_3,as}$  vibrations of acetate and the  $\nu_{\text{CH}}$  of formate indicate that both ions have a net orientation at the water surface with their CH bonds pointing toward the air phase. Furthermore, the  $\text{Im}[\chi^{(2)}]$  spectrum of acetate in  $\text{H}_2\text{O}$  shows a positive band at  $3000 - 3500\text{ cm}^{-1}$  that can be assigned to hydrogen-bonded OH stretch vibrations. The positive sign of the OH stretch band implies that the interfacial water molecules have a net orientation with their hydrogen atoms pointing toward the air, which can be explained from the negative charge of the acetate ions at the interface. The  $\text{Im}[\chi^{(2)}]$  spectrum of formate in  $\text{H}_2\text{O}$  a weak negative band in the frequency region  $3000 - 3500\text{ cm}^{-1}$ . The amplitude of this band is smaller than for neat water surface. The weak response of formate solutions in the frequency region  $3000 - 3500\text{ cm}^{-1}$  indicates that the water molecules have no clear net reorientation close to the surface upon the addition of the formate ions, which can be explained from the smaller surface propensity of formate compared to acetate. This finding is in line with previous surface tension measurements that show a negligible change in surface tension of formate solutions. In Figure 6 we also observe that for a solution of 4.5 m acetate the free O-H peak at  $3700\text{ cm}^{-1}$  is no longer present while it is still observed for a solution of 4.5 m formate. This observation can be explained from the fact that for a solution of 4.5 m acetate the surface concentration of carboxylate ions is much higher than for a solution of formate. This is also in line with previous surface tension measurements showing that for aqueous acetate solutions surface tension decreases with increased acetate content, which is



not the case for formate solutions. In addition, in the case of acetate adsorbed to the surface, a methyl group is sticking out of the surface, which is a much bulkier group than the C-H group of formate. Hence, for an aqueous solution of 4.5 m formate, much more room is left at the surface for dangling (free) water O-H groups than for an aqueous solution of 4.5 m acetate.

## Orientation of the carboxylate group at the water/air interface

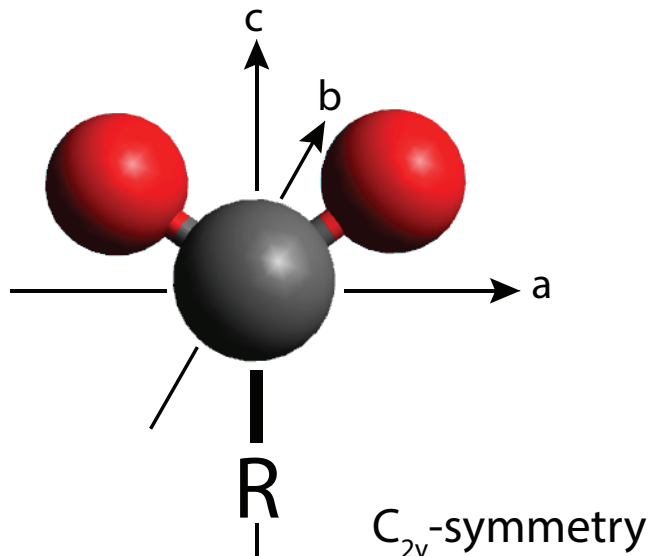


Figure 7: Molecular coordinate system for carboxylate group. The c-axis coincides with the rotation axis.

To estimate the tilt angle  $\theta$ , we performed auxiliary measurements in SPS polarization combination. Combining these data with SSP polarization data, the tilt angle can be estimated based on the response of the  $\nu_{as}$  vibration. The effective second-order susceptibility components detected in SSP and SPS polarization combinations are proportional to the components expressed in the laboratory coordinate system:

$$\chi_{SSP}^{(2),eff} \propto \chi_{xxz}^{(2),as} = \chi_{yyz}^{(2),as}, \quad (1)$$

$$\chi_{SPS}^{(2),eff} \propto \chi_{xxx}^{(2),as} = \chi_{yzy}^{(2),as} = \chi_{zyy}^{(2),as} = \chi_{zxx}^{(2),as} \quad (2)$$

In Figure 7 we show a schematic of the molecular coordinate system. The carboxylate group belongs to the  $C_{2v}$  symmetry group and thus possesses seven non-vanishing molecular

hyperpolarizability tensor elements:

$$\beta_{aac}, \beta_{bbc}, \beta_{ccc}, \beta_{aca} = \beta_{caa}, \beta_{bcb} = \beta_{cbb} \quad (3)$$

The four elements ( $\beta_{aca}, \beta_{caa}, \beta_{bcb}, \beta_{cbb}$ ) contribute to the  $\nu_{as}$  mode. Performing the Euler transformation and assuming free rotation of the carboxylate group around the molecular c-axis, the  $\chi^{(2)}$  components are described with the following expressions:<sup>3,4</sup>

$$\chi_{xxz}^{(2),as} = \chi_{yyz}^{(2),as} = -\frac{1}{2}N_s\beta_{aca}(\langle\cos\theta\rangle - \langle\cos^3\theta\rangle) \quad (4)$$

where  $N_s$  is surface population and  $\theta$  is the angle between the molecular c-axis and the normal to the interface. For SPS polarization combination the  $\chi^{(2)}$  components are described by:

$$\chi_{xxz}^{(2),as} = \chi_{yzy}^{(2),as} = \frac{1}{2}N_s\beta_{aca}\langle\cos^3\theta\rangle \quad (5)$$

for the antisymmetric mode. To extract the tilt angle, we assume that the products of the sample Fresnel coefficients are close when SSP and SPS polarization combinations are compared. Additionally, the quartz effective susceptibility components that are used for referencing have been reported to be close when SSP and SPS polarization combinations are probed.<sup>2</sup> By combining the expressions (2) and (3) we obtain the following relation between the experimentally observed amplitudes of the  $\nu_{as}$  mode measured with SSP and SPS:

$$\frac{\chi_{SSP}^{(2),as}}{\chi_{SPS}^{(2),as}} = -\frac{\langle\cos\theta\rangle - \langle\cos^3\theta\rangle}{\langle\cos^3\theta\rangle} \quad (6)$$

In Figure 8a we show the imaginary spectra measured for a 4.5 m sodium formate solution. While a strong response of  $\nu_{as}$  is observed with SSP, no distinct response of this vibration can be seen with SPS. Considering equation (6), this is most likely due to a tilt angle that is significantly larger than to  $45^\circ$ , as for this angle the amplitude measured with SPS is much

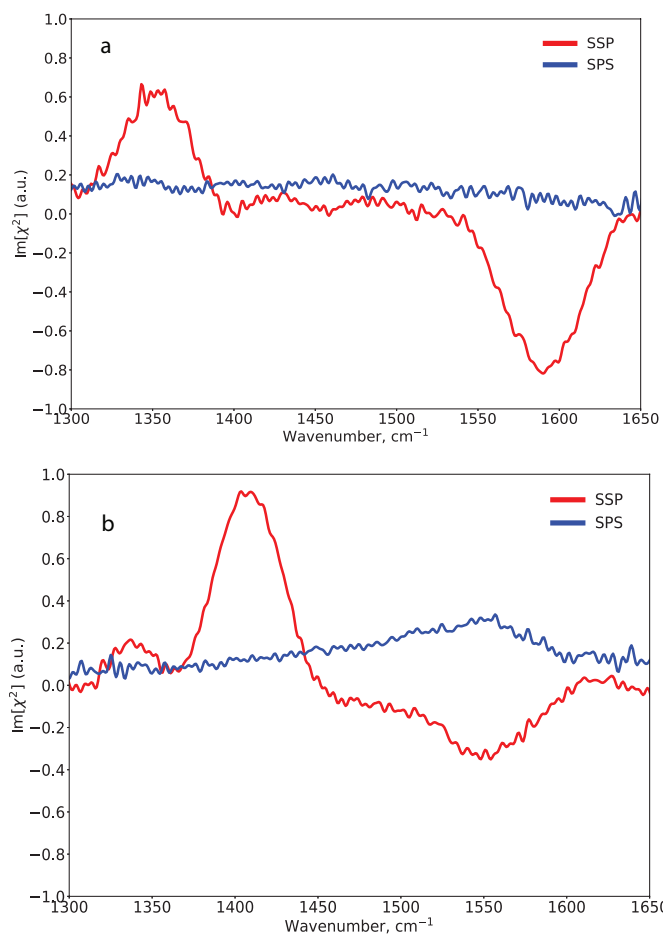


Figure 8:  $\text{Im}[\chi^{(2)}]$  spectra of a) 4.5 m sodium formate  $\text{D}_2\text{O}$  solution b) 2.5 m sodium acetate  $\text{D}_2\text{O}$  solution detected with SSP and SPS polarization combinations

smaller than the amplitude measured with SSP. When  $\theta$  increases to  $90^\circ$ ,  $\langle \cos^3\theta \rangle$  goes faster to zero than  $\langle \cos\theta \rangle$ . At the same time, the angle is expected to be smaller than  $90^\circ$  according to the  $\text{Im}[\chi^{(2)}]$  spectra measured in  $3 \mu\text{m}$  region shown on Figure 6.

In Figure 8b similar spectra are shown for a 2.5 m sodium acetate solution. We observe an almost equal response of the  $\nu_{as}$  vibration in both polarization combinations. In this case, the right-hand side of the equation (6) becomes equal to -1. To extract a value for the center of the angular distribution, the values  $\langle \cos\theta \rangle$  and  $\langle \cos^3\theta \rangle$  need to be calculated by integrating over the angular distribution.

We assume the angular distribution to be Gaussian distribution. This distribution becomes a  $\delta$ -distribution when the full-width-at-half-maximum (FWHM) of the distribution equals 0. In that limit no integration is required, and we directly obtain  $\theta = 45^\circ$ . We explore the dependence of the right-hand side of the equation (6) on the FWHM of the distribution, considering the central angle to be  $45^\circ$  by integrating the terms over the distribution.

As can be seen from Figure 9 the numerator and the denominator of the right-hand side of equation (6) have an almost identical dependence on the FWHM of the angular distribution up to a FWHM of this distribution of  $50^\circ$ . Hence, although we do not know the width of the angular distribution, the central value of this distribution of  $45^\circ$  is a quite robust number.

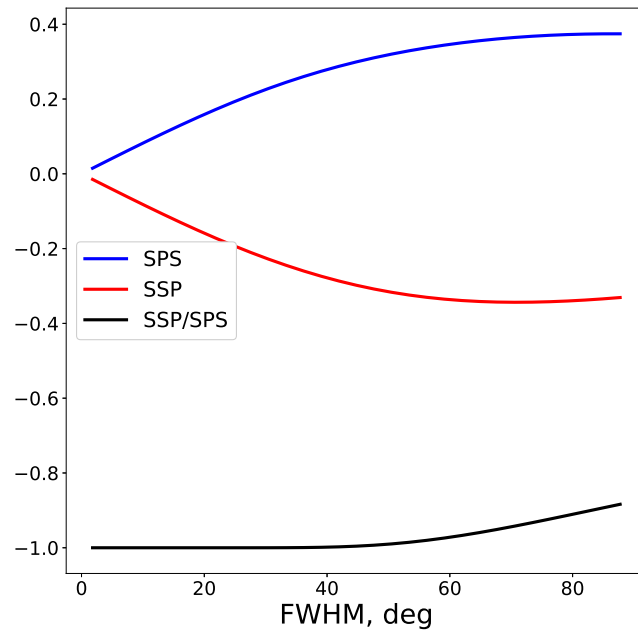


Figure 9: Dependence of the angular terms of expression (6) on the FWHM of the Gaussian distribution. Note that the numerator of the expression is proportional to the SSP signal while the denominator is proportional to the SPS signal

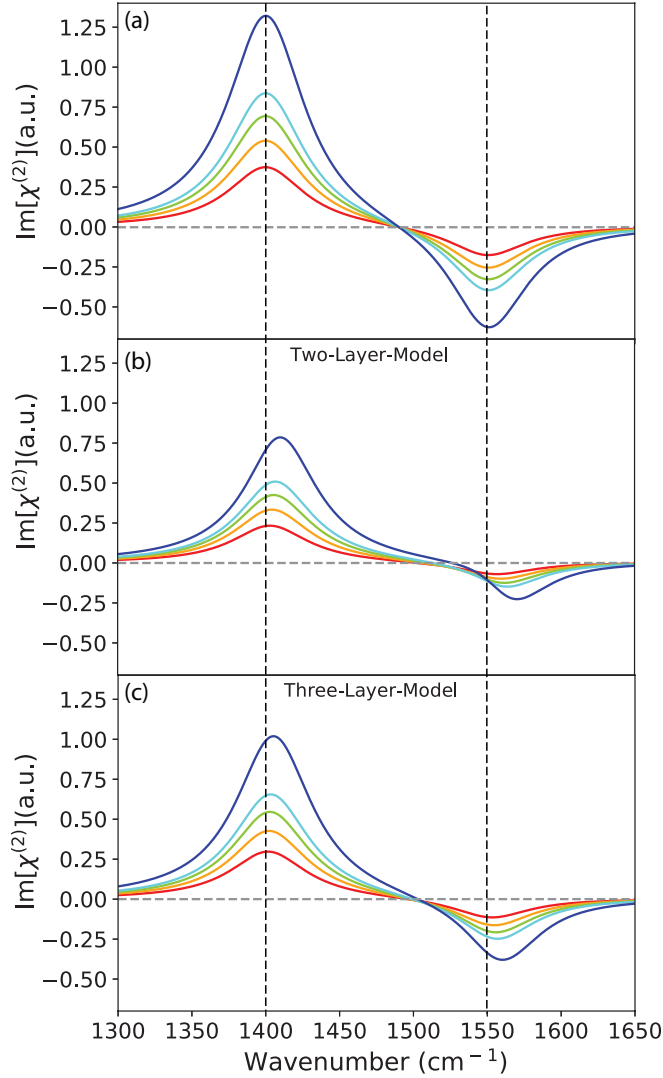


Figure 10: Modelling the effect of the Fresnel-Factors on the  $\nu_s$  and  $\nu_{as}$  vibrations of the carboxylate group for increasing concentrations.

Here, we model the vibrational responses of the  $\nu_s$  and  $\nu_{as}$  vibrations of the carboxylate group for acetate including the effect of the Fresnel factors on the vibrational response with increasing concentration. We use two different models: the two-layer model and the three-layer model.<sup>5,6</sup> Comparing the results of the two models with the experimental data we conclude that the two-layer model is overestimating the effects of the concentration dependent Fresnel factors, while the three-layer model is describing the shift of the vibrational

features very well.



## References

- (1) Ito, K.; Bernstein, H. J. the Vibrational Spectra of the Formate, Acetate, and Oxalate Ions. *Canadian Journal of Chemistry* **1956**, *34*, 170–178.
- (2) Hu, X.-H.; Wei, F.; Wang, H.; Wang, H.-F. -Quartz Crystal as Absolute Intensity and Phase Standard in Sum-Frequency Generation Vibrational Spectroscopy. *The Journal of Physical Chemistry C* **2019**, *123*, 15071–15086.
- (3) Wang, H. F.; Gan, W.; Lu, R.; Rao, Y.; Wu, B. H. Quantitative spectral and orientational analysis in surface sum frequency generation vibrational spectroscopy (SFG-VS). *International Reviews in Physical Chemistry* **2005**, *24*, 191–256.
- (4) Hirose, C.; Akamatsu, N.; Domen, K. Formulas for the analysis of surface sum-frequency generation spectrum by CH stretching modes of methyl and methylene groups. *The Journal of Chemical Physics* **1992**, *96*, 997–1004.
- (5) Morita, A. *Theory of Sum Frequency Generation Spectroscopy*; Springer: Singapore, 2018.
- (6) Wang, L.; Murata, R.; Inoue, K.-i.; Ye, S.; Morita, A. Dispersion of Complex Refractive Indices for Intense Vibrational Bands . II . Implication to Sum Frequency Generation Spectroscopy Published as part of The Journal of Physical Chemistry virtual special issue “ Dor Ben-Amotz Festschrift ” . **2021**,